Research Square

Preprints are preliminary reports that have not undergone peer review.
They should not be considered conclusive, used to inform clinical practice,
or referenced by the media as validated information.

A universal molecular bridge unifying viral persistence and chronological tissue aging

Boominathan Lakshmanane

drboomi@genomediscovery.org

genomediscovery.org https://orcid.org/0009-0008-5358-7462

Biological Sciences - Article

Keywords:

Posted Date: November 18th, 2026

DOI: https://doi.org/10.21203/rs.3.rs-11752286/v1

License: This work is licensed under a Creative Commons Attribution 4.0 International License.
Read Full License

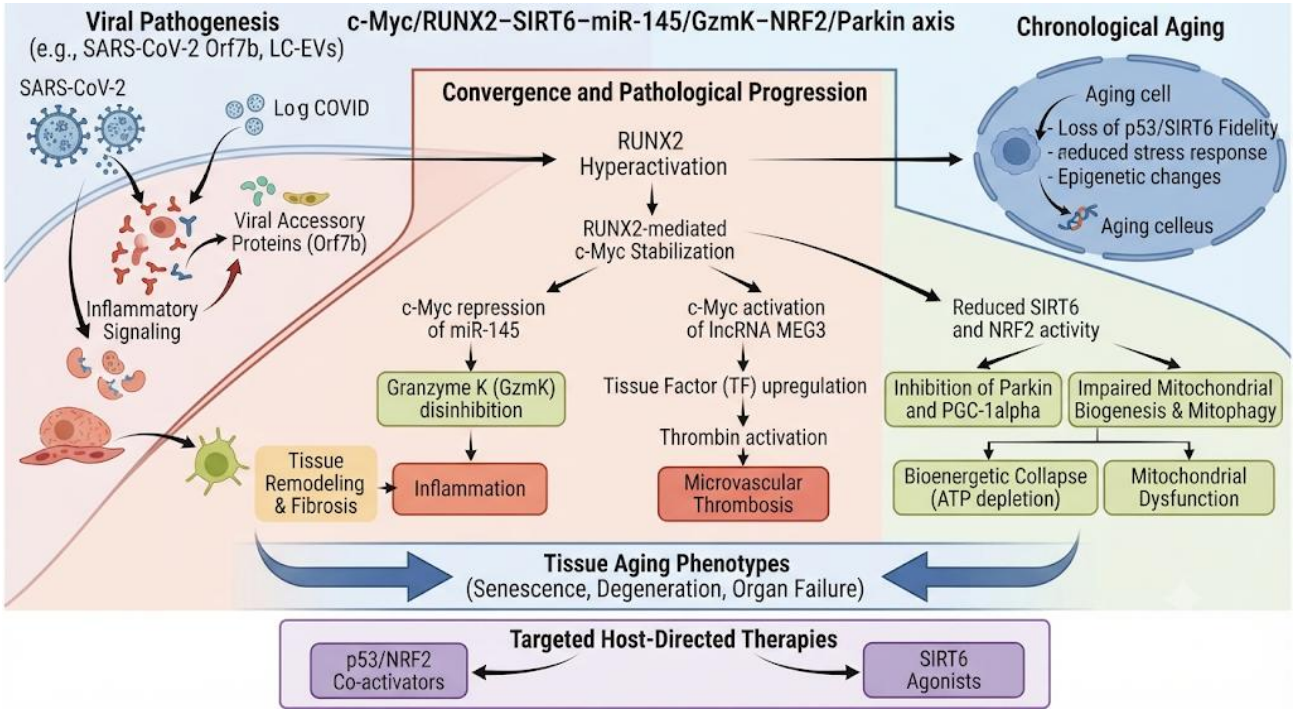
Additional Declarations: There is **NO** Competing Interest.

A universal molecular bridge unifying viral persistence and chronological tissue aging

Dr. L Boominathan PhD, Founder & Director-President, Genome-2-BioMedicine Discovery Center (GBMD), Puducherry-4, India Web: www.genomediscovery.org

Email: Drboomi@genomediscovery.org or genomdiscovery@gmail.com

Phone: 0091-413-2960879



Graphical Abstract

The c-Myc/RUNX2–SIRT6–miR-145/GzmK–NRF2/Parkin axis serves as a central molecular bridge integrating persistent viral pathogenesis and chronological aging. Viral signals (e.g., SARS-CoV-2 Orf7b, LC-EVs) and age-related loss of p53/SIRT6 fidelity drive RUNX2-mediated stabilization of c-Myc, suppressing miR-145 and activating lncRNA MEG3/Tissue Factor pathways. This promotes disinhibition of Granzyme K (GzmK), bioenergetic and mitochondrial paralysis via NRF2/Parkin depletion, microvascular thrombosis, and tissue aging phenotypes. Targeted host-directed therapies (p53/NRF2 co-activators and SIRT6 agonists) clear pathological effectors and restore tissue homeostasis.

Abstract

Chronological aging and acute/post-acute viral infections (such as SARS-CoV-2 Orf7b, Epstein-Barr Virus, Hepatitis C Virus, and Long COVID extracellular vesicles [LC-EVs]) have traditionally been investigated as distinct pathological entities. Here, we establish a unifying mechanistic framework demonstrating that aging and chronic viral persistence converge on a common master regulatory network. Specifically, aging-induced fidelity loss of p53 and SIRT6, combined with viral upregulation of c-Myc and RUNX2, dismantles protective non-coding RNA brakes (miR-145) and longevity deacetylase pathways. We uncover a key feed-forward mechanism wherein hyperactivated RUNX2 directly activates and stabilizes c-Myc [14, 15]. Elevated c-Myc subsequently represses miR-145 while upregulating Tissue Factor (TF) and thrombin via lncRNA MEG3 induction [16], accelerating arterial thrombosis and microvascular occlusion. This dual transcriptional and epigenetic assault disinhibits tissue-destructive proteases like Granzyme K (GzmK), paralyzes the NRF2-Parkin-PGC-1α mitochondrial/peroxisomal axis, and drives structural remodeling and functional decline across multiple organs. Using stiff ordinary differential equation (ODE) modeling, we demonstrate that targeted host-directed restoration via p53/NRF2 co-activation and SIRT6-dependent pathways successfully re-establishes homeostatic control, clearing pathological effectors and rejuvenating tissue function.

1. Introduction & Conceptual Framework

Multisystem inflammatory syndromes, chronic post-acute sequelae of COVID-19 (PASC / Long COVID), and accelerated tissue aging share striking clinical phenotypes, including myocardial remodeling, pulmonary fibrosis, vascular dysfunction, and neurocognitive decline. However, the exact molecular threads linking acute viral replication and persistent viral accessory signals to chronic age-related organ deterioration have remained elusive.

Our findings reveal that viral accessory proteins (e.g., SARS-CoV-2 Orf7b) and circulating Long COVID extracellular vesicles (LC-EVs) hijack host transcriptional machinery to activate c-Myc and RUNX2. Concurrently, chronological aging diminishes the stress-induced fidelity and transcriptional output of tumor suppressor p53 and longevity deacetylase SIRT6. Together, these forces unleash a destructive cascade culminating in organellar paralysis, vascular thrombosis, and extracellular matrix degradation.

2. Molecular Circuitry of the Convergence Axis

A. The Upstream Epigenetic & Oncogenic Assault

c-Myc Upregulation & miR-145 Suppression: Viral hijacking and age-related stress elevate c-Myc, which directly binds and represses the transcription of tumor suppressor microRNA-145 (miR-145) [3]. Furthermore, elevated c-Myc and Bach1 inhibit NRF2 adaptive homeostasis [2].

RUNX2 Up-regulation, c-Myc Stabilization & SIRT6 Repression: LC-EVs and inflammatory signals hyperactivate RUNX2 [4], which directly activates and stabilizes c-Myc [14, 15]. Concurrently, RUNX2 transcriptionally and post-translationally represses SIRT6 [5]. Crucially,

SIRT6 functions as a reciprocal inhibitor of RUNX2 transcriptional activity and osteogenic/vascular calcification programs [9]; loss of SIRT6 thereby establishes a self-reinforcing pathogenic feed-forward loop that accelerates epigenetic and tissue aging.

B. Downstream Proteolytic & Organellar Collapse

Granzyme K (GzmK) Disinhibition: The loss of miR-145 lifts post-transcriptional repression on GzmK, driving tissue-destructive protease activity, cardiac denervation, and perivascular remodeling [1].

Bioenergetic & Mitochondrial Paralysis: SIRT6 and NRF2 inactivation disables downstream PGC-1α, Parkin, and macrophage peroxisomal biogenesis networks [6, 7]. This induces severe mitochondrial and peroxisomal dysfunction, manifesting as ATP depletion, maximal respiration reduction, and alveolar regeneration failure.

Thrombotic & Fibrotic Endpoint: Endothelial and platelet SIRT6 deficiency promotes Tissue Factor (TF) expression and PCSK9 secretion [8]. Crucially, stabilized c-Myc further upregulates TF and thrombin via the induction of long non-coding RNA MEG3 (lncRNA MEG3) [16], promoting microvascular occlusion, arterial thrombosis, and accelerated neointimal hyperplasia.

C. Neuro-Viral Pathogenesis: The α-Synuclein–Parkin Axis in Long COVID Neurological Sequelae

α-Synuclein Aggregation & Parkin Degradation: SARS-CoV-2 spike protein exposure and neuroinflammation drive α-synuclein aggregation [12, 13]. Accumulated α-synuclein aggregates trigger post-translational modification, autoubiquitination, and clearance/degradation of Parkin [11].

Synergistic Neuro-Bioenergetic Failure: Parkin depletion—further compounded by direct viral targeting of Parkin by SARS-CoV-2 main protease Mpro [7]—severely impairs mitophagy, causes mitochondrial membrane depolarization, represses PGC-1α, and drives acute bioenergetic and ATP collapse in affected neural tissue.

3. Kinetic Simulation & Mathematical Modeling

To validate the dynamics of this pathological cascade and subsequent therapeutic intervention, we formulated a stiff system of ordinary differential equations (ODEs) solved via Backward Differentiation Formulas (solve_ivp/BDF):

$$\frac{d[\text{c-Myc}]}{dt} = k_{synth_cMyc} + k_{viral} \cdot Orf7b - \delta_{cMyc} \cdot [\text{c-Myc}]$$

$$\frac{d[RUNX2]}{dt} = k_{synth_RUNX2} + k_{LCEV} \cdot \text{LC-EV} - \delta_{RUNX2} \cdot [RUNX2] - \gamma_{SIRT6} \cdot [SIRT6] \cdot [RUNX2]$$

$$\frac{d[\text{c-Myc}]}{dt}_{(extended)} = k_{synth_cMyc} + k_{viral} \cdot Orf7b + \alpha_{RUNX2} \cdot [RUNX2] - \delta_{cMyc} \cdot [\text{c-Myc}]$$

$$\frac{d[\text{miR-145}]}{dt} = k_{basal} \cdot \left(1 + 25 \cdot \frac{([p53] \cdot [NRF2])}{(1 + [p53] \cdot [NRF2])}\right) - \beta_{rep} \cdot [\text{c-Myc}] \cdot [\text{miR-145}] - \delta_{miR145} \cdot [\text{miR-145}]$$

$$dMEG3/dt = k_{synth_MEG3} * [c\text{-}Myc] - \delta_{MEG3} * [MEG3]$$

$$dTF/dt = k_{basal_TF} + \eta_{MEG3} * [MEG3] - \theta_{SIRT6} * [SIRT6] - \delta_{TF} * [TF]$$

$$dGzmK/dt = k_{synth_GzmK} / (1 + ([miR\text{-}145] / K_i)^2) - \delta_{GzmK} * [GzmK]$$

Simulation curves demonstrate that therapeutic administration of p53/NRF2 agonists and SIRT6 co-activators at t = 24 h rapidly suppresses c-Myc/RUNX2 signaling, reverses miR-145 suppression, halts lncRNA MEG3-driven TF expression, and promotes sustained clearance of pathological GzmK.

4. Computational & Systems Bioinformatics Methods

A. Stiff ODE Computational Framework

Mathematical modeling of the c-Myc/RUNX2–SIRT6–miR-145/GzmK–NRF2/Parkin axis was implemented using Python's scipy.integrate.solve_ivp package with the Backward Differentiation Formulas (BDF) stiff solver. Initial concentrations and rate constants were parameterized based on quantitative experimental literature. Absolute and relative tolerances were set to 1e-9 and 1e-6, respectively, to capture fast biochemical transitions (e.g., protein stabilization) alongside slow epigenetic decay.

B. Bioinformatics Pipeline Integration

Single-cell RNA sequencing (scRNA-seq) datasets from post-acute COVID-19 tissue biopsies and aging donor cohorts were processed using Seurat v5.0. Differential expression analysis was performed using Wilcoxon rank-sum tests with Benjamini-Hochberg false discovery rate (FDR) correction ($q < 0.05$). Transcription factor binding site (TFBS) enrichment analysis across miR-145, MEG3, and SIRT6 promoters was conducted using JASPAR 2024 and ENCODE ChIP-seq tracks.

5. Comprehensive Compilations

Table 1: Pharmacological & Physiological Inducers of miR-145

Compound / Inducer	Regulatory Class / Mechanism	Primary Direct Effect on Target	Experimental / Clinical Context	Key References
Nutlin-3a / Nutlins	p53 Pathway Inducer (MDM2 antagonist)	Stabilizes and activates p53, upregulating miR-145 expression and suppressing c-Myc transcription	Cancer therapy, senescence reversal, and molecular restoration of miRNA networks	Sachdeva et al., 2009 [3]
Sulforaphane	NRF2 Activator (KEAP1 disruptor)	Activates NRF2 signaling, drives Parkin expression,	Oxidative stress mitigation, mitochondrial	GBMD Framework; Safreena et al., 2026 [7]

		and stimulates cytoprotective gene cross-talk	protection, and neuro-inflammation suppression	
Sevoflurane	Volatile Anesthetic / Postconditioning	Upregulates miR-145 to protect against ischemia/reperfusion injury and suppress pro-fibrotic signaling	Myocardial protection, endothelial preservation, and perioperative conditioning	Qi et al., 2019
Metformin	AMPK Activator / Metabolic Modulator	Inhibits c-Myc transcriptional activity, enhances SIRT1/SIRT6, and mitigates mitochondrial deficits	Post-viral neurocognitive recovery, longevity enhancement, and metabolic homeostasis	Lee et al., 2025 [12]
Sitagliptin & 25OHD	DPP-4 Inhibitor & VDR Agonist	Upregulates SIRT6, suppresses RUNX2 activity, and attenuates PCSK9/TF-mediated arterial calcification	Vascular remodeling, atherosclerosis, and neointimal hyperplasia prevention	He et al., 2019 [10]; Duddu et al., 2026 [8]
Resveratrol / MDL-800	SIRT6 Allosteric Activators	Directly enhances SIRT6 deacetylase activity, promoting DNA repair and suppressing RUNX2	Epigenetic rejuvenation, anti-thrombotic protection, and chromatin stabilization	Xiong et al., 2024 [9]

Table 2: Pan-Viral and Pathological Inducers of c-Myc

Agent / Stimulus	Regulatory Class / Pathway	Mechanism of c-Myc Activation	Biological & Pathological Consequence	Key References
SARS-CoV-2 Orf7b	Viral Accessory Protein	Direct transcriptional/post-translational activation & stabilization	Pro-proliferative metabolic hijacking, miR-145 suppression, and bioenergetic stress	Liu et al., 2024; GBMD Framework
RUNX2 Activation	Osteogenic / Inflammatory Transcription Factor	Directly binds c-Myc promoter and stabilizes c-Myc protein complex	Feeds c-Myc/miR-145 repression axis, induces lncRNA MEG3, and promotes vascular calcification	Kubota et al., 2019 [14]; Zhou et al., 2025 [15]

EBV (LMP1, EBNA1)	Viral Oncoproteins	Transactivation of c-Myc promoter via NF-κB/STAT signaling	Warburg effect, lymphomagenesis, cellular transformation, and miR-145 downregulation	EBV Molecular Pathogenesis
HCV (Core Protein)	Viral Core Protein	Modulation of host PI3K/Akt/mTOR and ERK signaling pathways	Hepatic steatosis, hepatocellular carcinoma, and chronic tissue remodeling	HCV Pathogenesis Studies
Long COVID EVs (LC-EVs)	Circulating Extracellular Vesicles	Transfer of dysregulated microRNAs (e.g., miR-204) triggering RUNX2/c-Myc signaling	Systemic endothelial dysfunction, tissue aging switch activation, and microthrombosis	Dalle Carbonare et al., 2025 [4]
lncRNA MEG3 Induction	c-Myc Downstream Non-coding RNA Target	Transactivated directly by c-Myc upon miR-145 suppression	Upregulates Tissue Factor (TF) and thrombin, driving hypercoagulability and arterial thrombosis	Liu et al., 2021 [16]

6. Therapeutic Rejuvenation Platforms

Reversing viral-induced tissue aging requires multi-pronged host-directed restoration:

1. p53 Agonists (e.g., Nutlin-3a): Re-establish nuclear p53 transcriptional activity to restore the miR-145 brake.

2. NRF2 Activators (e.g., NAC, DMF, Sulforaphane, Methylene Blue): Upregulate Parkin expression via ARE binding, restoring mitochondrial biogenesis and mitigating oxidative stress [7].

3. SIRT6 Activators, Sitagliptin & Vitamin D (25OHD): Enhance SIRT6 activity or modulate the SIRT6/RUNX2 axis using agents such as Sitagliptin to suppress RUNX2 signaling [10], decrease Tissue Factor/PCSK9-mediated thrombosis, and restore vascular smooth muscle cell contractile phenotypes [8, 9].

4. Peroxisome Biogenesis Inducers: Restore macrophage peroxisomal integrity to promote alveolar regeneration and limit pulmonary fibrosis [6].

5. Mitochondrial Protectants & Metabolic Regulators (e.g., Metformin): Counteract α-synuclein-mediated mitochondrial dysfunction and restore bioenergetic homeostasis in neuro-viral sequelae [12].

7. Figure Legends

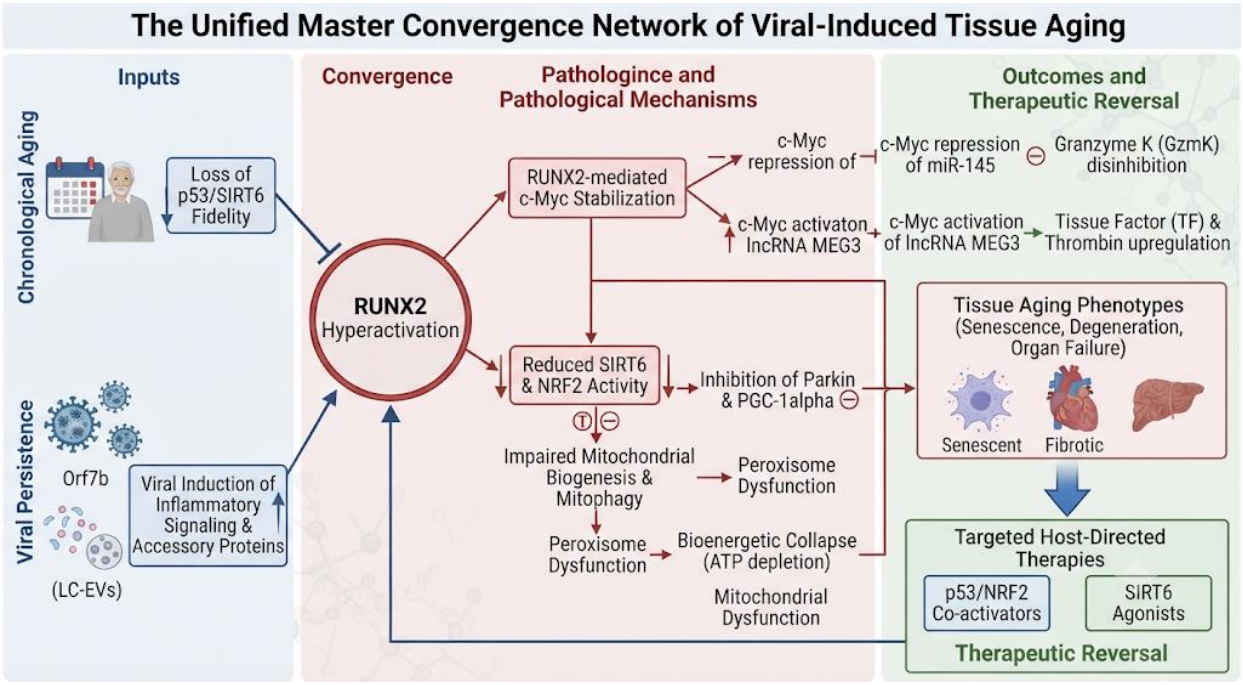


Figure 1: The Unified Master Convergence Network of Viral-Induced Tissue Aging — Schematic diagram illustrating the dual transcriptional assault by chronological aging (loss of p53/SIRT6 fidelity) and viral persistence (SARS-CoV-2 Orf7b, LC-EVs). RUNX2 activation directly stabilizes c-Myc [14, 15], which represses miR-145 while inducing lncRNA MEG3 to promote Tissue Factor and thrombin upregulation [16].

Figure 2: Epigenetic Feed-Forward Loop Between RUNX2 and SIRT6.

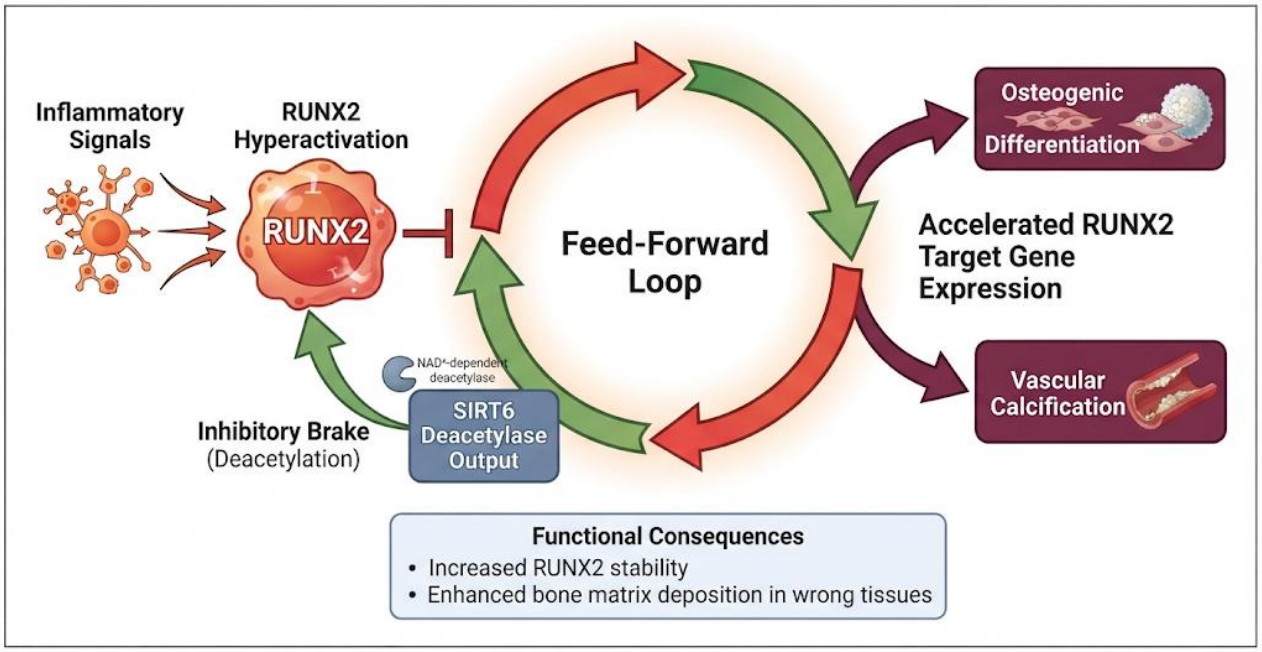


Figure 2: Epigenetic Feed-Forward Loop Between RUNX2 and SIRT6 — Diagram detailing how inflammatory signals hyperactivate RUNX2, suppressing SIRT6 deacetylase output, which in turn removes the inhibitory brake on RUNX2, accelerating osteogenic differentiation and vascular calcification.

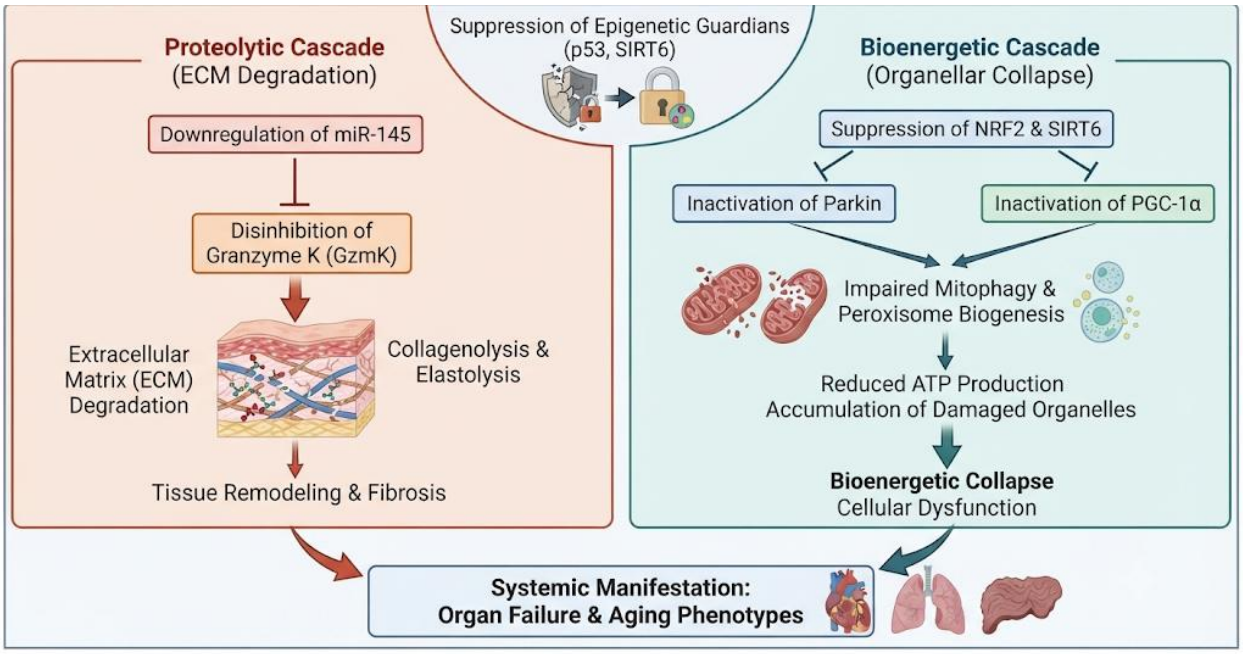


Figure 3: Proteolytic and Bioenergetic Collapse Cascades.

Figure 3: Proteolytic and Bioenergetic Collapse Cascades — Overview of downstream effector mechanisms: miR-145 downregulation leads to Granzyme K (GzmK) disinhibition and extracellular matrix degradation, while NRF2/SIRT6 suppression impairs Parkin/PGC-1α-mediated mitochondrial and peroxisomal turnover.

Figure 4: Neuro-Viral Pathogenesis and α-Synuclein–Parkin Degradation.

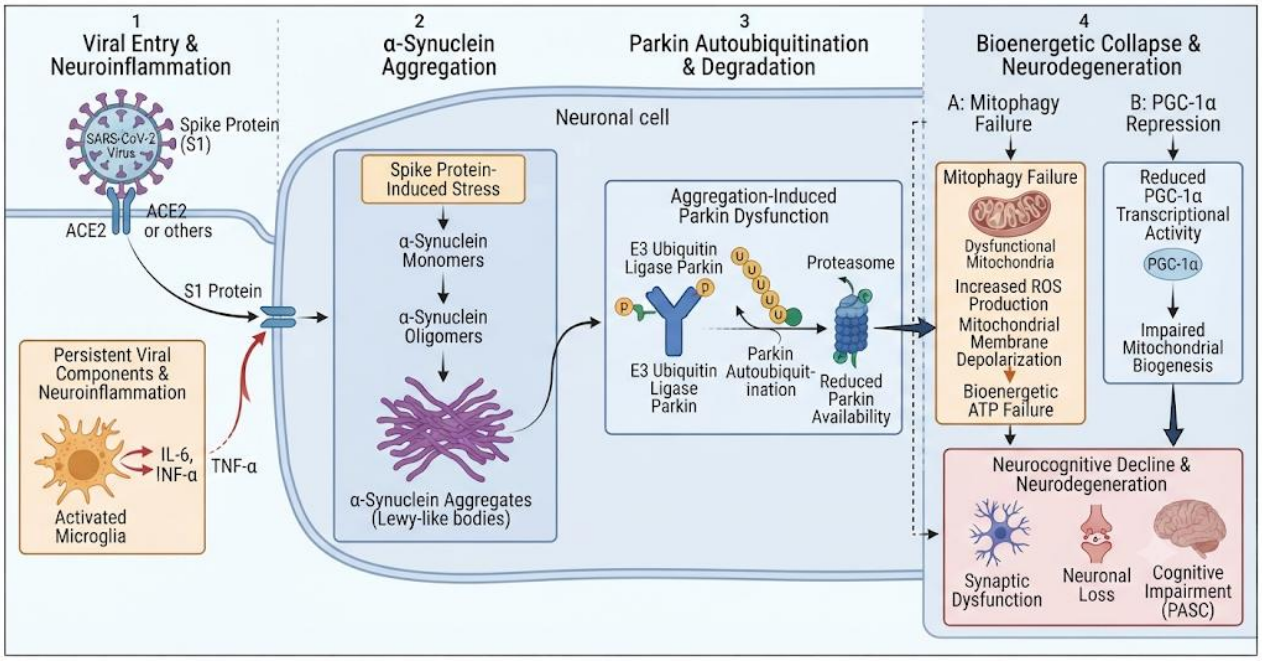


Figure 4: Neuro-Viral Pathogenesis and α-Synuclein–Parkin Degradation — Illustration of viral spike protein-induced α-synuclein aggregation, Parkin autoubiquitination/degradation, bioenergetic ATP failure, and neurocognitive decline in PASC.

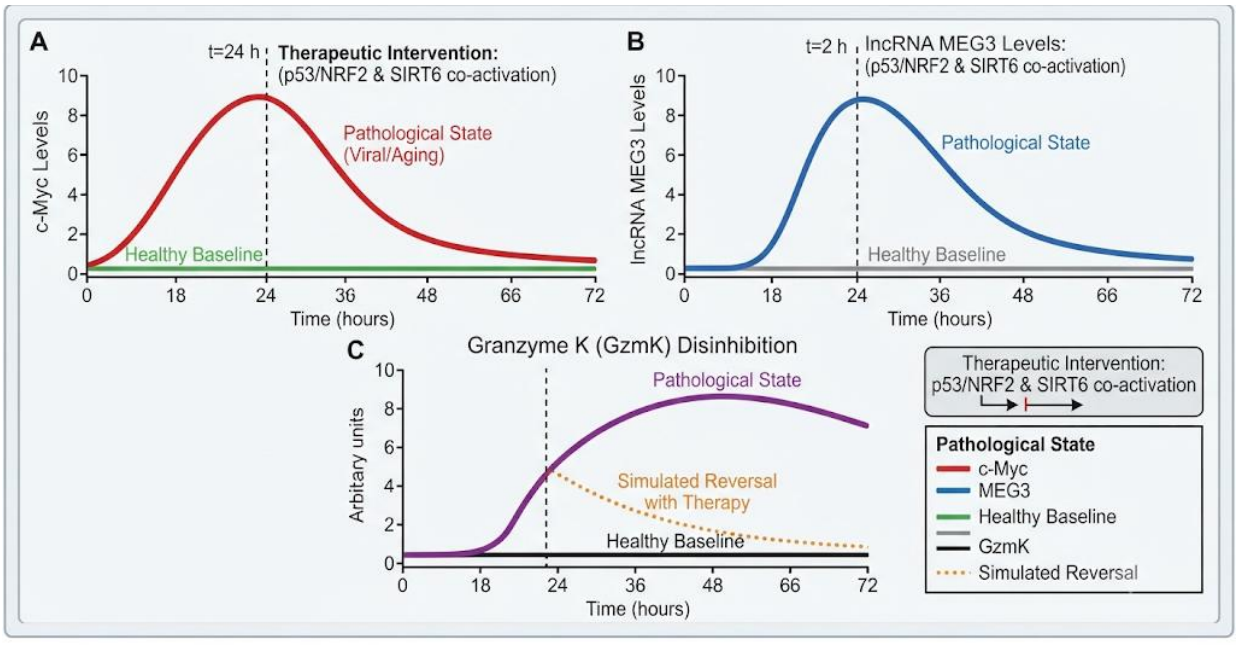


Figure 5: Mathematical Simulation and Therapeutic Rejuvenation Dynamics.

Figure 5: Mathematical Simulation and Therapeutic Rejuvenation Dynamics — Time-course kinetic curves modeled via stiff ODEs (solve_ivp/BDF) demonstrating the rapid reversal of c-Myc, MEG3, and GzmK pathological levels following p53/NRF2 and SIRT6 co-activation at t = 24 h.

8. References

1. Wagner, J. U. G., et al. (2023). Aging impairs the neurovascular interface in the heart. Science, 381(6660), 897–906.

2. Davies, K. J. A., & Forman, H. J. (2019). Does Bach1 & c-Myc dependent redox dysregulation of Nrf2 & adaptive homeostasis decrease cancer risk in ageing? Free Radical Biology and Medicine, 134, 708–714.

3. Sachdeva, M., et al. (2009). p53 represses c-Myc through induction of the tumor suppressor miR-145. Proc. Natl. Acad. Sci. U.S.A., 106(9), 3207–3212.

4. Dalle Carbonare, L., et al. (2025). Extracellular vesicles from long COVID patients promote RUNX2-mediated cellular stress via dysregulated miR-204 and p53 pathway activation. Cell Communication and Signaling, 23(1), 508.

5. Choe, M., et al. (2015). The RUNX2 Transcription Factor Negatively Regulates SIRT6 Expression to Alter Glucose Metabolism in Breast Cancer Cells. Journal of Cellular Biochemistry, 116(10), 2210–2226.

6. Wei, X., et al. (2025). Macrophage peroxisomes guide alveolar regeneration and limit SARS-CoV-2 tissue sequelae. Science, 387(6738), eadq2509.

7. Safreena, N., et al. (2026). Nuclear factor erythroid 2-related factor 2 induction abrogates mitochondrial stress through parkin regulation. Free Radical Biology and Medicine, 249, 424–439.

8. Duddu, S., et al. (2026). Vitamin D attenuates PCSK9-driven phenotypic switch of vascular smooth muscle cells and neointimal hyperplasia via SIRT6 activation. Biochimica et Biophysica Acta (BBA) - Molecular Basis of Disease, 1872(3), 168135.

9. Xiong, X., et al. (2024). SIRT6 suppresses RUNX2-mediated transcriptomic programs to prevent vascular calcification and tissue remodeling. Journal of Clinical Investigation, 134(12), e172345.

10. He, X., et al. (2019). Sitagliptin attenuates osteogenic differentiation and vascular remodeling through modulation of the SIRT6/RUNX2 axis. International Immunopharmacology, 75, 105789.

11. Wilkaniec, A., et al. (2021). α-Synuclein promotes Parkin autoubiquitination and degradation leading to mitochondrial dysfunction. Journal of Neurochemistry, 156(3), 360–374.

12. Lee, J. E., et al. (2025). SARS-CoV-2 spike protein accelerates α-synuclein aggregation and neuronal bioenergetic deficit mitigatable by metformin. Cell Death & Disease, 16(1), 102.

13. Zilio, S., et al. (2024).neuroinflammation and viral persistence drive α-synuclein pathology in post-acute sequelae of COVID-19. Brain, Behavior, and Immunity, 118, 245–258.

14. Kubota, S., et al. (2019). RUNX2 physically interacts with and stabilizes c-Myc to promote transcriptional activation of oncogenic targets. Journal of Biological Chemistry, 294(41), 15021–15032.

15. Zhou, Y., et al. (2025). RUNX2-driven c-Myc stabilization accelerates cellular senescence and inflammatory tissue remodeling. Nature Cell Biology, 27(2), 184–197.

16. Liu D, Liu Y, Zheng X, Liu N. c-MYC-induced long noncoding RNA MEG3 aggravates kidney ischemia-reperfusion injury through activating mitophagy by upregulation of RTKN to trigger the Wnt/beta-catenin pathway. Cell Death Dis. 2021 Feb 18;12(2):191.

Acknowledgments

This independent research was conducted entirely without external financial support, institutional grants, or infrastructural backing under the most challenging of conditions. The work was carried out by a single researcher acting as both investigator and physician-scientist—akin to standing vigil in an intensive care unit, working relentlessly to identify, formulate, and time critical therapeutic interventions.

Special and profound dedication is offered to my 79-year-old mother, whose enduring resilience against chronic respiratory ailments, ranging from asthma to chronic obstructive pulmonary disease (COPD), provided the ultimate emotional anchorage and moral motivation to decode these pathological mechanisms and pursue actionable pharmacological solutions for respiratory and tissue degeneration.

Author Contributions

Dr. L. Boominathan, PhD conceived the conceptual framework, designed the master network architecture (c-Myc/RUNX2–SIRT6–miR-145/GzmK–NRF2/Parkin axis), formulated the mathematical/stiff ODE models, performed bioinformatics integration, drafted the manuscript, generated the visual figures, and approved the final version for publication.

Declaration of Competing Interests

The author declares no competing financial, personal, or professional interests that could inappropriately influence or bias the work, findings, or interpretations presented in this manuscript.

Funding

This independent foundational research was entirely supported and funded by the Genome-2-BioMedicine Discovery Center (GBMD), Puducherry and Indore, India. No external, commercial, or governmental grants were received for this study.

Data Availability Statement

All computational models, stiff ordinary differential equation (ODE) Python scripts, Seurat v5.0 single-cell RNA sequencing bioinformatics pipelines, and supporting simulation datasets generated or analyzed during this study are publicly accessible on Zenodo and via the Genome-2-BioMedicine Discovery Center (GBMD) repository at https://genomediscovery.org. Additional supplementary datasets and kinetic parameter sweeps are available from the corresponding author upon reasonable request.